

Q-factor: A measure of competition between the topper and the average in percolation and in SOC

Asim Ghosh¹, S. S. Manna^{2,*} and Bikas K. Chakrabarti^{3,4}

¹*Department of Physics, Raghunathpur College, Raghunathpur 723133, India*

²*B-1/16 East Enclave Housing, 02 Biswa Bangla Sarani, New Town, Kolkata 700163, India*

³*Saha Institute of Nuclear Physics, Kolkata 700064, India*

⁴*Economic Research Unit, Indian Statistical Institute, Kolkata 700108, India*

We define the Q -factor in the percolation problem as the quotient of the size of the largest cluster and the average size of all clusters. As the occupation probability p is increased, the Q -factor for the system size L grows systematically to its maximum value $Q_{max}(L)$ at a specific value $p_{max}(L)$ and then gradually decays. Our numerical study of site percolation problems on the square, triangular and the simple cubic lattices exhibits that the asymptotic values of p_{max} though close, are distinctly different from the corresponding percolation thresholds of these lattices. We have also shown using the scaling analysis that at p_{max} the value of $Q_{max}(L)$ diverges as L^d (d denoting the dimension of the lattice) as the system size approaches to their asymptotic limit. We have further extended this idea to the non-equilibrium systems such as the sandpile model of self-organized criticality. Here, the $Q(\rho, L)$ -factor is the quotient of the size of the largest avalanche and the cumulative average of the sizes of all the avalanches; ρ being the drop density of the driving mechanism. This study has been prompted by some observations in Sociophysics.

I. INTRODUCTION

Critical fluctuations of all length scales appearing at the critical points are the signatures of phase transitions. Over the last century, extensive studies of phase transitions have helped establishing the statistical physics descriptions of the scaling theory and the critical phenomena in different physical systems. For example, few well studied systems are magnetic and fluid systems [1], polymer systems [2], [3] for percolating systems [3], and Self-organized Critical (SOC) systems [4]. Essentially, the order parameter of the corresponding systems vanish following in general a singular power law or critical behavior at the critical point and beyond. Its higher moments include susceptibilities, diverge again with singular or critical power law exponent values at the respective critical points. For SOC systems, these singular behaviors are seen from the pre-critical side and then remains critical in the SOC state of the systems. For practical purposes, these diverging susceptibilities help locating the critical point.

For social systems, scientists had studied for ages, starting with Pareto law 80-20 law [5], Lorenz function [6], Gini index [7], Hirsch index [8], etc., the extreme unequal distributions of income or wealth, votes, paper citations respectively. Following some recent observations [9–11] of extreme inequality level in citation statistics of successful individuals and even institutions / universities / journals, with Gini and other inequality index values going beyond the Pareto 80-20 limit, we studied and found [12] clear presence of similar level of the inequality index values in the physical models of SOC system, like

the Bak, Tang, Wiesenfeld (BTW) sandpile [13] and the Manna [14] sandpile. Particularly, in our recent study [15] of the citation statistics of some very successful prize winning scientists and a few others not so successful scientists it has been observed that their research dynamics is clearly SOC like and most successful have achieved the critical level in their citation inequalities, while others are still approaching that level, though they have not reached there. All these studies showed, just the average high level of citations per paper (reflected by the Hirsch index values, which are determined by the effective network coordination or Dunbar number [16, 17] do not reflect the success of the scientist, but the high level (beyond the Pareto level) of critical fluctuations in citations from publication to publication of the scientist. Indeed, it was seen in [15] that crossing a threshold value of a simple quotient of the citation number of the highest cited paper and the average citation of all the papers (including the highest cited one) by the scientist gives very good correlation with the appreciations by the respective communities.

Following this clue, we study here how the topper competes with the average in the well known models of percolation processes and in the sandpile model of self-organized criticality. In the percolation model we have defined the Q -factor as the quotient of the largest cluster size and the average size over all clusters for the percolation models. Similarly, the Q -factor in the sandpile model has been defined as the quotient of the largest avalanche size and the average size over all avalanches. As the control variables are tuned in these problems Q -factors grow very sharply right before a specific value of the control variable, reaches the maxima, and then decay very rapidly. The locations of the maxima are distinctly different from the critical points of these systems.

We have described our calculations and results of the percolation problem for the square, triangular and the

*asimghosh066@gmail.com, subhrangshu.manna@gmail.com (corresponding author), bikask.chakrabarti@saha.ac.in

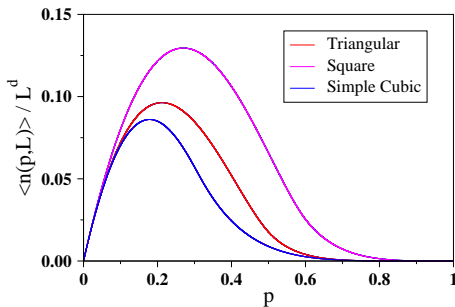


FIG. 1: Plot of the average number of distinct clusters per lattice site $\langle n(p, L) \rangle / L^d$ against the site percolation occupation probability p . For each type of lattice the data for three different system sizes are plotted which overlapped completely, only the colors used for the largest lattices are visible.

simple cubic lattices in the three sub-sections of section II. Here, we have calculated the Q -factors for the entire range of the occupation probability p . A nice finite-size extrapolation gives the precise value of the percolation occupation probability p_{max} in the asymptotic limit which we found to be larger than their percolation thresholds. In section III we have executed similar analysis for the BTW sandpile where we used the drop density ρ as the tuning parameter. The value of ρ_{max} in the asymptotic limit have been calculated. Finally, we have summarized in section IV.

II. SITE PERCOLATION

A. Square lattice

An initially empty square lattice of size $L \times L$ has been gradually filled in by occupying the randomly selected lattice sites one by one. At any arbitrary intermediate stage the fraction ‘ p ’ of occupied sites is referred as the percolation occupation probability. A cluster is defined as the set of occupied sites connected by nearest neighbour distances. Different distinct clusters have been identified using the well known Hoshen Kopelman algorithm [18]. Since we are not going to study any spanning property of the percolation clusters we have used the periodic boundary conditions in all simulations reported here. The number of distinct clusters $n(p, L)$ increases from unity at $p \rightarrow 0+$, reaches a maximum at some intermediate p value and then finally goes down to unity again at $p = 1$. We refer the entire process as a ‘run’.

In Fig. 1 we have plotted the average number of distinct clusters per lattice site $\langle n(p, L) \rangle / L^d$ against p for three different system sizes of the square, triangular, and the simple cubic lattices, where d represents the Euclidean dimensional of these lattices. The collapse of the plots on top of one another for three system sizes is extremely well. The sizes of the lattices used are $L = 256, 1024, \text{ and } 4096$ for the square and

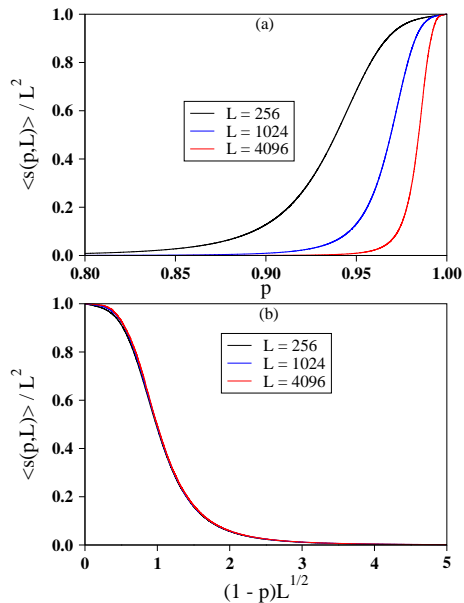


FIG. 2: (a) Plot of the average cluster size $\langle s(p, L) \rangle$ scaled by the total number L^2 of lattice sites against the site percolation occupation probability p for the square lattice. (b) The same data have been replotted against $(1 - p)L^{1/2}$ which yield nice collapse of the data.

triangular lattices, where as $L = 32, 64, \text{ and } 128$ for the simple cubic lattice. The peak positions of these curves have coordinates: (0.26968, 0.12954) for the square lattice, (0.21192, 0.096306) for the triangular lattice, and (0.17871, 0.086066) for the simple cubic lattice.

At an intermediate stage the average size of all clusters including the largest one is therefore $s_{av}(p, L) = pL^d / n(p, L)$. This is further averaged over a large number of independent runs and we define the average cluster size $\langle s(p, L) \rangle = \langle s_{av}(p, L) \rangle$. In Fig. 2(a) we have plotted the scaled average cluster size $\langle s(p, L) \rangle / L^2$ against p only for the square lattice and again for the same three system sizes. The curves become sharper as $p \rightarrow 1$ and as the system size becomes larger. In Fig. 2(b) we have inverted the x -axis and re-plotted the same data $\langle s(p, L) \rangle / L^2$ against $(1 - p)L^{1/2}$ to observe a nice collapse of the data over the entire range of p values.

As more and more sites are occupied, the growth of the size s_{max} of the largest cluster has been monitored. The order parameter $\Omega(p, L)$ of the percolation transition is defined as the fractional size of the largest cluster averaged over many independent runs, i.e., $\Omega(p, L) = \langle s_{max}(p, L) \rangle / L^d$. In Fig. 3 we have plotted the order parameter $\Omega_{sq}(p, L)$ for the square lattice for three different system sizes. Larger the system size, the growth of the order parameter becomes sharper. For a particular system $\Omega_{sq}(p, L)$ grows rapidly as the percolation occupation probability p approaches from below the site percolation threshold of the square lattice whose best value till date is $p_c(sq) = 0.59274605079210(2)$ [19, 20].

Now we define the Q -factor as the quotient of the av-

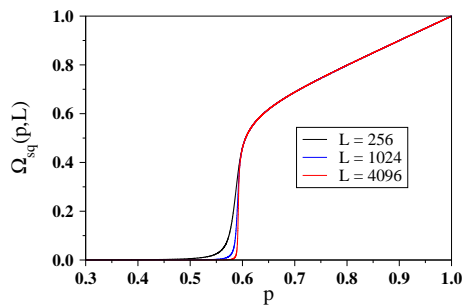


FIG. 3: Plot of the percolation order parameter $\Omega_{sq}(p, L) = \langle s_{max}(p, L) \rangle / L^2$ against the site percolation occupation probability p for the square lattice.

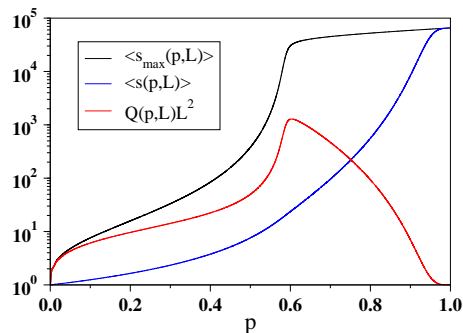


FIG. 4: Plot of the average size of the largest cluster $\langle s_{max}(p, L) \rangle$, average size of all clusters $\langle s(p, L) \rangle$, and the Q -factor $Q(p, L)L^2$ against the site occupation probability p for a system of size $L = 256$ on the square lattice.

average size $\langle s_{max}(p, L) \rangle$ of the largest cluster and the average size $\langle s(p, L) \rangle$ of all clusters for every value of p for a certain system size L as:

$$Q(p, L) = (\langle s_{max}(p, L) \rangle / \langle s(p, L) \rangle) / L^d \quad (1)$$

$$= \Omega(p, L) / \langle s(p, L) \rangle.$$

We have plotted in Fig. 4 three quantities for a particular system size $L = 256$. They are, (i) the average size $\langle s_{max}(p, L) \rangle$ of the largest cluster, (ii) the average size $\langle s(p, L) \rangle$ of all clusters, and (iii) the $Q(p, L)$ factor multiplied by the system size L^2 . The first two quantities are monotonically increasing functions of p . It is observed that when p gradually increases to a specific value $\langle p_{max}(L) \rangle$, the value of $\langle s_{max}(p, L) \rangle$ becomes increasingly larger than the average cluster size $\langle s(p, L) \rangle$ and therefore $Q(p, L)$ increases very sharply. However, after crossing $\langle p_{max}(L) \rangle$, the growth of $\langle s_{max}(p, L) \rangle$ becomes slower but $\langle s(p, L) \rangle$ maintains its previous growth rate. Consequently, their ratio Q -factor decays gradually which explains the existence of a peak of Q at $\langle p_{max}(L) \rangle$. This is visible in Fig. 5 where we have plotted $Q_{sq}(p, L)$ against p for three different system sizes. All three curves have single peaks of nearly the same heights but their positions have systematic variations.

Now we present numerical evidences in Fig. 6 to claim that the asymptotic value $p_{max} = \lim_{L \rightarrow \infty} \langle p_{max}(L) \rangle$ is

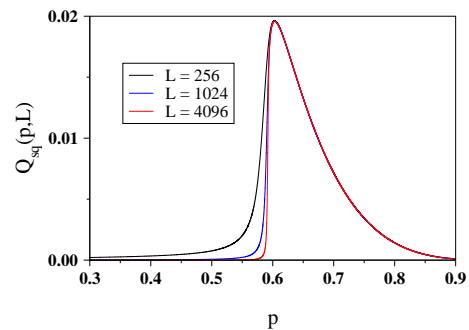


FIG. 5: Plot of $Q_{sq}(p, L)$ against the percolation occupation probability p for the square lattice.

distinctly different from the ordinary percolation threshold p_c on the same lattice. Let us denote a typical run from an empty lattice ($p = 0$) to a fully occupied lattice ($p = 1$) on the square lattice of size $L \times L$ by α . For every α we estimate three different values of the occupation probability, namely: (i) the value of occupation probability $p_c(\alpha, L)$ at which the occupation of only the next site in the sequence causes the maximal jump of the size of the largest cluster $s_{max}(\alpha, L)$; (ii) the value of $p_Q(\alpha, L)$ at which the occupation of only the next site in the sequence causes the maximal jump of the value of the $Q(\alpha, L)$ -factor, and (iii) the value of $p_{max}(\alpha, L)$ at which the ratio $s_{max}(\alpha, p, L) / s_{av}(\alpha, p, L)$ reaches its maximum value.

Their average values $\langle p_c(L) \rangle$, $\langle p_Q(L) \rangle$ and $\langle p_{max}(L) \rangle$ have been calculated over a large number of runs, namely 10^8 runs for lattices of size up to $L = 128$, which decreases to 18000 for $L = 4096$. Each of these quantities is then extrapolated using a finite size correction term in the power law form: $\langle p_c(L) \rangle = p_c - AL^{-1/\nu_k}$ where ν_1 , ν_2 and ν_3 correspond to p_c , p_Q and p_{max} respectively. Here, $\nu_1 = \nu$ the ordinary correlation length exponent of two dimensional percolation problem. In comparison to $1/\nu_1 = 0.75$ we get 0.7574, which is quite close. The values of $1/\nu_2 = 0.9145$ and $1/\nu_3 = 1.0425$ show that the values of ν_2 and ν_3 are quite different from ν , but their values are close to each other and nearly equal to 1.

After extrapolation the asymptotic value of $p_c = 0.592717$ has been obtained which is very close to the actual value of the site percolation threshold ≈ 0.592746 with a difference of ≈ 0.00003 . The asymptotic value of $p_Q = 0.592419$ has been found which is ≈ 0.0003 away from the percolation threshold. Where as, the asymptotic value of $p_{max} = 0.603288$ differs by an amount ≈ 0.01 from the percolation threshold. With this analysis, we conclude that while the values of p_Q and p_c are most likely to be the same, the value of p_{max} is infact, distinctly different from p_c .

In our next analysis we have calculated and plotted the ratios of successive values of three quantities. Specifically, if the occupation probability is increased by a small amount of say $\Delta p = 1/L^2$, i.e., one more site is occupied, then to what factors the quantities (i) $\langle s_{max}(p, L) \rangle$, (ii)

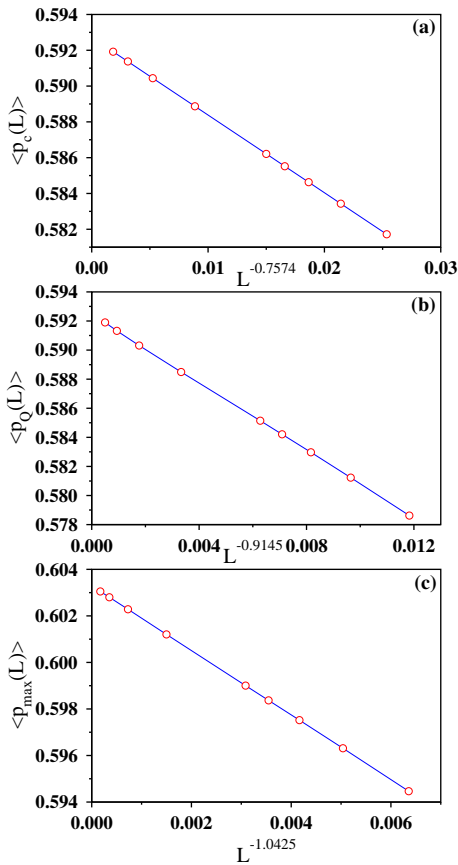


FIG. 6: Finite size extrapolations with suitable tuning parameters yield (a) $p_c = 0.592717$, $1/\nu_1 = 0.7574$; (b) $p_Q = 0.592419$, $1/\nu_2 = 0.9145$ and (c) $p_{max} = 0.603288$, $1/\nu_3 = 1.0425$.

$\langle s(p, L) \rangle$ and (iii) $Q(p, L)$ are increased? Let these ratios be denoted by

$$\begin{aligned} \mathcal{R}[\langle s_{max}(p, L) \rangle] &= \frac{\langle s_{max}(p+\Delta p, L) \rangle}{\langle s_{max}(p, L) \rangle}, \\ \mathcal{R}[\langle s(p, L) \rangle] &= \frac{\langle s(p+\Delta p, L) \rangle}{\langle s(p, L) \rangle}, \\ \mathcal{R}[Q(p, L)] &= \frac{\langle Q(p+\Delta p, L) \rangle}{\langle Q(p, L) \rangle} = \frac{\mathcal{R}[\langle s_{max}(p, L) \rangle]}{\mathcal{R}[\langle s(p, L) \rangle]} \end{aligned}$$

respectively and are plotted in Fig. 7 for $L = 256$. In Fig. 3 we find the size of the largest cluster increases very fast right before the percolation threshold, but right after the percolation it starts increasing with p approximately linearly. Therefore the $\mathcal{R}[\langle s_{max}(p, L) \rangle]$ must be having a peak at $p_c(L)$ and the black curve indeed shows a peak at $p_c(L = 256) \approx 0.579815$. From Fig. 2 we observed that the value of $\langle s(p, L) \rangle$ increases very slowly except when p is nearly equal to 1. Therefore, the curve in red in Fig. 7 exhibits the slow variation of $\mathcal{R}[\langle s(p, L) \rangle]$ against p . Consequently, their ratio $\mathcal{R}[Q(p, L)]$ (in blue) is also having a peak at p_c , and beyond this peak, it decreases systematically.

Two points are to be noticed: The Q -factor has its maximum at $p_{max}(L)$ where the ratio $\mathcal{R}[Q(p, L)]$ is equal to unity. Therefore, at $p = p_{max}(L)$ the two curves meet at point 1 where $\mathcal{R}[\langle s_{max}(p, L) \rangle] = \mathcal{R}[\langle s(p, L) \rangle]$. The

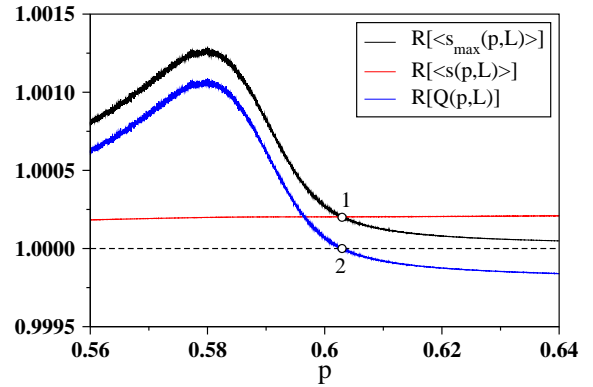


FIG. 7: Plots of $\mathcal{R}[\langle s_{max}(p, L) \rangle]$, $\mathcal{R}[\langle s(p, L) \rangle]$ and $\mathcal{R}[Q(p, L)]$ against the site occupation probability p for the square lattice of size $L = 256$. The first two curves meet at the point 1 where their values are equal. Therefore, their ratio is unity which corresponds to $\mathcal{R}[Q(p, L)] = 1$ at the point 2.

other point 2 on the $\mathcal{R}[Q(p, L)]$ against p plot represents the point $\mathcal{R}[Q(p_{max}, L)] = 1$. We argue, if $p_c(L)$ and $p_{max}(L)$ both assume the same asymptotic value i.e., $p_c = p_{max}$, it would mean a discontinuous drop in the values of $\mathcal{R}[Q(p)]$ at this value of p , which is not possible since both the largest and the average cluster sizes vary continuously in a continuous phase transition like the ordinary percolation.

We have calculated the error in our estimate for the asymptotic value of p_{max} . For a system of size L we have calculated the standard deviation $\sigma(L) = \{\langle p_{max}^2(L) \rangle - \langle p_{max}(L) \rangle^2\}^{1/2}$. We have plotted in Fig. 8(a) the values of $\sigma(L)$ against L using the double-logarithmic scale. We have observed that $\sigma(L)$ nicely scales as $L^{-0.658}$. Let us denote the number of independent runs be M , then we define the error as $e(L) = \sigma(L)/M^{1/2}$. For this plot the number of runs M varied from 24 million for $L = 128$ to 3000 for $L = 4096$. In the Fig. 8(b) of $\langle p_{max}(L) \rangle$ values have been plotted against $L^{-1.0363}$ and we have plotted errors using the vertical lines. For each point we have drawn a vertical line from $\langle p_{max}(L) \rangle - e(L)$ to $\langle p_{max}(L) \rangle + e(L)$ and then two horizontal bars of fixed length at the two ends of the vertical line (a zoomed plot of only the two points for $L = 2048$ and 4096 has been shown for clarity in the inset). It is obvious that the errors are really small. We will conclude the maximal error in the estimation of the asymptotic value of p_{max} quite possibly is 0.0002 and therefore our final estimate is $p_{max} = 0.6033 \pm 0.0002$ which is distinctly different from the actual value of $p_c \approx 0.592746$.

We have also tried a log correction to the finite-size correction as follows:

$$\langle p_{max}(L) \rangle = p_{max} - AL^{-\alpha}(1 - B(\ln L/L)). \quad (2)$$

From our best fit we obtained $p_{max} = 0.60329$, $A = 1.4323$, $\alpha = 1.047$ and $B = 0.2608$ which shows that the log correction has very little effect on p_{max} (figure not shown).

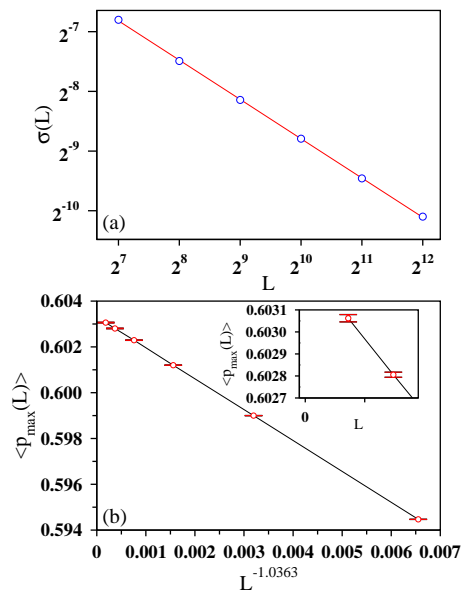


FIG. 8: (a) The standard deviation $\sigma(L)$ for the values of $p_{max}(L)$ of the square lattice have been plotted against the system size L on the log – log scale. The estimation of slope implies $\sigma(L) \sim L^{-0.658}$. (b) The average values of $\langle p_{max}(L) \rangle$ have been plotted against $L^{-1.0363}$ to obtain a nice straight line. Each point is marked with its error bar. The extrapolated value of $p_{max} = 0.6033 \pm 0.0002$ has been obtained.

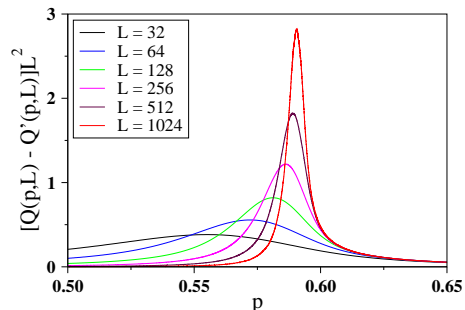


FIG. 9: The difference $\Delta Q = [Q(p, L) - Q'(p, L)]L^2$ have been plotted for six different sizes of the square lattice against the site occupation probability p .

The collapse of the peak positions $Q_{max}(p_{max}, L)$ of the curves in Fig. 5 on one another implies the maximal cluster size at this point $\langle s_{max}(L) \rangle \sim L^\eta$ with $\eta = 2$. This has been directly verified by plotting (figure not shown) $\langle s_{max}(L) \rangle$ against L using the double logarithmic scales for the square and simple cubic lattices. The values of the exponent η have been estimated from the slopes of the curves. For the square lattice $\eta_{sq} = 2.0057$ has been obtained and for the simple cubic lattice $\eta_{sc} = 3.0075$ is found. This implies that since $\langle p_{max} \rangle$ values are slightly larger than the percolation thresholds, the largest clusters turn out to be compact, and not fractals like the percolating clusters at the percolation thresholds. Consequently, their dimensions are equal to their embedding space dimensions. This analysis gives another support to

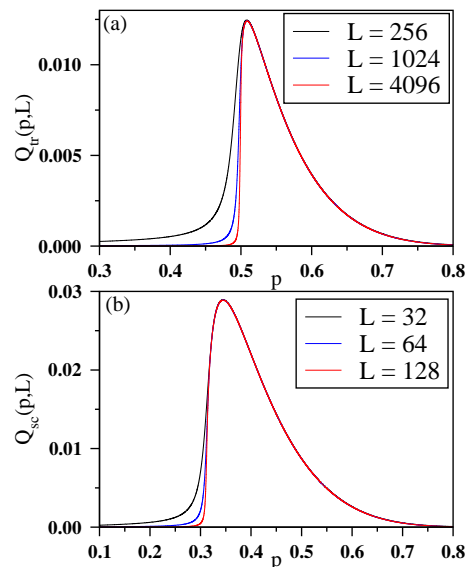


FIG. 10: Plots of the Q -factors against the site occupation probability p for two different lattices: (a) $Q_{tr}(p, L)$ for the triangular lattice and (b) $Q_{sc}(p, L)$ for the simple cubic lattice.

our claim that p_c and p_{max} are indeed distinctly different. An alternate definition of Q -factor is as follows:

$$Q'(p, L) = \langle (s_{max}(p, L) / s_{av}(p, L)) \rangle / L^d. \quad (3)$$

Here, for each value of p of every run, one first calculates the quotient of the largest cluster size $s_{max}(p, L)$ and the average cluster size $s_{av}(p, L)$ and then takes an average of this quotient over a large number of independent runs.

We have calculated both the $Q(p, L)$ and $Q'(p, L)$ -factors for the same set of runs. When we plot these two Q -factors against p on the same graph, it appears with the naked eye that one curve completely overlaps the other as if the two factors are equal. Actually this is not the case which becomes apparent when we plotted the difference $\Delta Q = [Q(p, L) - Q'(p, L)]L^2$ against p in Fig. 9 for six different sizes of the square lattice. It is observed that though the maximal value of the difference is very small, there is a nice peak for ΔQ occurring at $\langle p_{max}(L) \rangle$. The number of independent runs varied from 10^8 up to $L = 64$ to 320000 for $L = 1024$. The locations of the maxima i.e., p_{max} and p'_{max} for $Q(p, L)$ and $Q'(p, L)$ respectively are almost always the same, if not, they differ by an amount $\sim 1/L^2$. They are extrapolated as $\langle p_{max}(L) \rangle = 0.603312 - Const.L^{-2.1429}$.

B. Triangular lattice

A parallel set of calculations have been done on the triangular lattice. A plot of $Q_{tr}(p, L)$ against p for three different system sizes have been shown in Fig. 10(a). The positions of the maxima are very close to the triangular lattice percolation threshold $p_c = 1/2$ but slightly larger

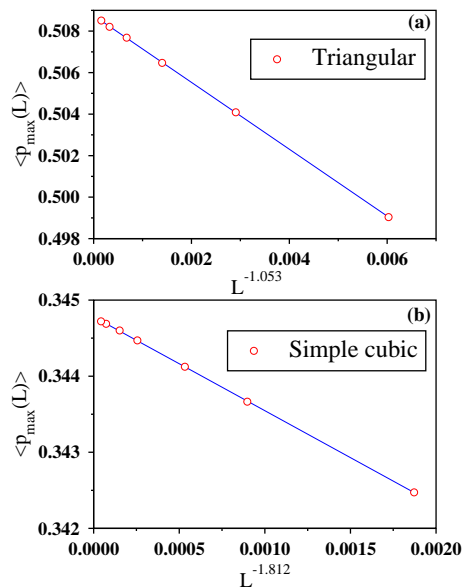


FIG. 11: Extrapolation of $\langle p_{max}(L) \rangle$ values to their asymptotic limit of $L \rightarrow \infty$ gives the estimates of p_{max} : (a) 0.5088 for the triangular lattice, and (b) 0.3448 for the simple cubic lattice.

than $1/2$. For each run we have estimated the maximum value of $Q_{max}(p_{max}, L)$, the corresponding p_{max} values and then averaged over all runs. The average $\langle p_{max}(L) \rangle$ values of six different system sizes from $L = 128, \dots, 4096$ have been extrapolated to their asymptotic limit: $\langle p_{max}(L) \rangle = p_{max} - const.L^{-1.053}$ with $p_{max} = 0.5088$ which is approximately 0.9 percent different from the percolation threshold $p_c = 1/2$, see Fig. 11(a).

C. Simple Cubic lattice

For the simple cubic lattice we could study only small lattice sizes up to $L = 256$ and plot them in Fig. 10(b). The only difference for the simple cubic lattice is the quotient of the maximal size and average size is scaled by L^3 , that is the total number of lattice sites in the system.

$$Q_{sc}(p, L) = (\langle s_{max}(p, L) \rangle / \langle s(p, L) \rangle) / L^3. \quad (4)$$

The data for the positions of the maximum of $Q_{sc}(p, L)$ for the lattice sizes $L = 32$ to 256 have been used to extrapolate $\langle p_{max}(L) \rangle = p_{max} - const.L^{-1.812}$ with $p_{max} = 0.3448$ (Fig. 11(b)).

Therefore, in each of the three lattices, namely, square, triangular and simple cubic we see that the precise values of the probabilities p_{max} are about 1% larger than their corresponding percolation thresholds p_c . Clear power laws for the finite-size extrapolations in Fig. 6 and in Fig. 11 in all three cases indicate that indeed these threshold values p_{max} are distinctly different from their p_c values. These extrapolations are characterized by the exponents

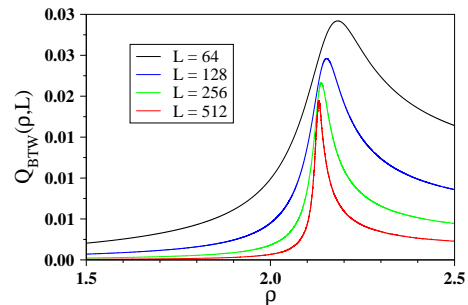


FIG. 12: For the BTW sandpile the values of $Q_{BTW}(\rho, L)$ have been plotted against the average number of sand particles ρ dropped per site of a square lattice.

whose values are very close, namely, 1.041 for the square lattice and 1.053 for the triangular lattice and widely different 1.812 for the simple cubic lattice which may be the indication of universality of the finite-size correction exponent. It may be that more extensive study in future with much larger systems would yield values 1 and 2 for these exponents in two and three dimensions, a possibility which we cannot rule out at this moment. Our conclusion that p_{max} are different, has also been supported by the independent measurements of the average mass of the largest clusters at $p_{max}(L)$ which yield that indeed these clusters are of compact structures instead of being fractals at their percolation thresholds. Here we like to recall another problem of percolation connectivity between two points at distance of separation of the order of the system size [21]. There also enhanced thresholds for the percolation connectivities of the modified structure have been observed.

III. BTW SANDPILE

The Bak, Tang, and Wiesenfeld (BTW) sandpile [13] has been studied on the square lattice of size $L \times L$ with open boundary condition. The dynamical evolution of the sandpile starts from a completely empty lattice. Sand particles are dropped one by one at randomly selected lattice sites. The system is allowed to relax through the deterministic BTW sandpile dynamics [13]. The avalanche created by dropping one particle has size s , measured by the total number of sand column topplings in the avalanche. At any arbitrary intermediate stage of the sandpile dynamics, let ρ be the average number of sand particles dropped per lattice site. We refer it as the ‘drop density’ which is a measure of the net inward current of sand mass. This implies that an average number of ρL^2 particles have been dropped on to the system, many of which have left the system by jumping outside through the boundary. Therefore, the drop density ρ of particle addition is the control variable in this problem.

We have kept track of the maximal size $s_{max}(\rho, L)$ of all the avalanches created till ρL^2 particles have been

dropped. At the same time we have also calculated the cumulative average size $s_{av}(\rho, L)$ of all the avalanches of sizes larger than zero, including the largest avalanche. Each run consists of a sequence of particle drops till the system moves well inside the stationary regime. We have checked that running the simulation till the drop density reaches a value of $\rho = 2.5$ ensures arrival to the stationary state. Quantities which are averaged over many such independent runs are denoted by the angular brackets $\langle \dots \rangle$. Finally, we have defined a Q -factor which is the quotient of the largest avalanche size and the average avalanche size of the sandpile:

$$Q_{BTW}(\rho, L) = (\langle s_{max}(\rho, L) \rangle / \langle s_{av}(\rho, L) \rangle) / L^2 \quad (5)$$

and plot this quantity against the drop density ρ in Fig. 12. There is a nice peak of value $Q_{max}(L)$ at the position $\rho_{max}(L)$ which we measure for four different system sizes. The rise and fall of $Q_{BTW}(\rho, L)$ values on the two sides of $\rho_{max}(L)$ are found to be asymmetric. Therefore, the variation of $Q(\rho, L)$ against ρ around the drop density $\rho_{max}(L)$ has a λ -shape and the peak becomes sharper as the system size becomes larger. In the sub-critical regime, sizes of all avalanches are small, so the value of Q is small and ~ 1 . The moment the system moves into the stationary regime a very large avalanche abruptly appears which is quite generic in all sandpile models. This makes the value of s_{max} in the numerator quite large, but in comparison the value of s_{av} in the denominator increases only a little since all the avalanches share this increase in the total sum of all the avalanches. This results in a rapid increase of Q . Beyond the drop density $\rho_{max}(L)$ the system moves into the stationary state where the s_{max} increases very slowly, but s_{av} increases very fast to reach a steady value. This ensures that after the peak $Q(\rho, L)$ takes a stationary value as both the numerator and denominator assume steady values. This explains the λ -shape of the peak.

For a single sequence of sand grain additions on a system of size L , let $\rho_{max}(L)$ be the precise value of the average number of particles dropped per site of the lattice corresponding to the maximum value $Q_{max}(\rho, L)$ of the Q -factor of Eqn. 5. We have calculated $\langle \rho_{max}(L) \rangle$ using two different methods and plotted them against two different negative powers of L in Fig. 13(a). (i) Red: For each run we have picked up the maximum value $Q_{max}(\rho, L)$ of Q and its corresponding drop density ρ_{max} . These two quantities are then averaged over a large number of independent runs. It has been observed that both $\langle \rho_{max}(L) \rangle$ and $\langle Q_{max}(\rho, L) \rangle$ depend on the system size L (Fig. 13(b)). The best values of the exponents for extrapolation of these two quantities are selected using the least square fit method and the straight lines are then extrapolated to the $L \rightarrow \infty$ limit. We found $\langle \rho_{max}(L) \rangle = 2.127 + 5.95L^{-1.12}$ and $\langle Q_{max}(L) \rangle = 0.023 + 0.136L^{-0.44}$. (ii) Blue: Using a large number of runs and we have calculated for each value of ρ the value of $\langle s_{max}(\rho, L) \rangle$ and $\langle s_{av}(\rho, L) \rangle$ and then calculated $Q(\rho, L)$ using Eqn. 5. The maximum

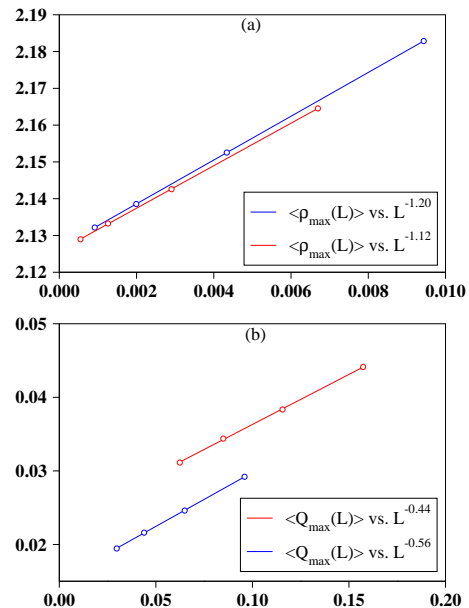


FIG. 13: For the BTW sandpile (a) the drop densities $\langle \rho_{max}(L) \rangle$ for the maximal Q -factors and (b) the average values of the maximal Q -factors $\langle Q_{max}(L) \rangle$ have been plotted against different negative powers of L . The two colors, red and blue, represent two different ways of calculations. The extrapolated values in the asymptotic limit of $L \rightarrow \infty$ are consistent with each other.

value $Q_{max}(\rho, L)$ have been determined and its location $\rho_{max}(L)$ have been estimated. They are again best fitted by the least square method and then extrapolated. We found $\langle \rho_{max}(L) \rangle = 2.126 + 5.78L^{-1.20}$ and $\langle Q_{max}(L) \rangle = 0.015 + 0.147L^{-0.56}$.

IV. SUMMARY

How far the topper was ahead of a typical student in your class? One way to answer this question may be possible by looking at the total marks obtained in the final examination. Similarly how the richest in the society is ahead of the average members can be estimated by looking at their wealth. Thirdly, how the most famous research paper of a reputed scientist enjoys the maximum credit compared to the average credit of all his papers can be gauged by looking at his updated list of citation indices. Quite possibly one can cite more examples where the credit of the topper is compared with the average credit of the of a typical individual.

All these examples are dynamic in nature, e.g., the identification of the topper and the marks secured by him changes from one exam to the other. Identity of the richest may also change from a year to the next, and so also the citations received by the best paper of the scientist. Therefore, we thought it to be the best to consider a so-called ‘competition’ between the topper and the average and quantify this by defining the quotient of their credits

as the Q -factor. The natural question that comes to the mind, is why this study is important at all? The reason is this factor is a quantitative measure of the fluctuations of the marks obtained by the students, wealth possessed by different members of the society, or the quality of the papers written by the scientist.

We would like to recall that the citation statistics of majority scientists indicated growth of fluctuations in citations with time. For very “successful” scientists, the statistical measures seem to indicate that these fluctuations reach an universal SOC level. It was also observed that for a successful scientist the ratio of the citation number of the highest cited paper to the average citation of all his papers often takes a value beyond a threshold (peak) value. In comparison, the value of the same ratio for not so reputed scientists do not reach that desired level.

This observation gave us the clue that the behavior of quotient of the largest to the average credits may be interesting to study in other physical systems as well. Therefore, in this paper we have decided to apply this idea to systems well known in statistical physics. One example is the problem of percolation from the equilibrium systems and the other one is the sandpile model of self-organized criticality from the non-equilibrium systems. Both the systems evolve under suitably defined dynamical rules. One defines the ‘connected clusters’ in the percolation process and the ‘avalanche clusters’ in the sandpile model analogous to the group of members in the society. Though these systems in their early stages are un-correlated, under the process of evolution they gradu-

ally become correlated. The signature of the correlation is traced in the rapid growth of the largest cluster in the percolation process and the largest avalanche in the sandpile model. The credits possessed by these members are estimated by the cluster sizes and the avalanche sizes.

In both the examples, the system passes through a transition point. On increasing the site occupation probability the percolating system makes a transition from the sub-critical to super-critical phase through the critical point. At this point the size of the largest cluster grows at the fastest rate compared to the average size of all cluster. However, immediately after the percolation transition the rate of growth of the largest cluster slows down. As a consequence the Q -factor exhibits a peak at a specific value of the site occupation probability p_{max} which is about $\sim 1\%$ larger than the percolation threshold p_c of all lattices. We have argued in the text that these two numbers p_{max} and p_c cannot be the same, only because of the fact that the percolation transition is a continuous transition. A very similar scenario arises for the sandpile model where the current size of the largest avalanche undergoes a large jump in its size when the system moves into the self-organized stationary state.

Acknowledgement

We are very much thankful to Amnon Aharony and Robert Ziff for their insightful comments and suggestions. BKC is grateful to the Indian National Science Academy for their Senior Scientist Research Grant.

-
- [1] H. E. Stanley, Introduction to Phase Transitions and Critical Phenomena, Oxford University Press Clarendon, Oxford (1971).
- [2] P. G. De Gennes, Scaling Concepts in Polymer Physics, Cornell University Press, Ithaca, N.Y. (1979).
- [3] D. Stauffer and A. Aharony, Introduction to Percolation Theory, Taylor & Francis, London, Philadelphia (1991).
- [4] P. Bak, How Nature Works: The Science of Self-Organized Criticality, Copernicus. New York (1996).
- [5] V. Pareto, Cours d’Economie Politique, Lausanne, Rouge (1897).
- [6] M. O. Lorenz, (1905) Methods of measuring the concentration of wealth, Publications of the American Statistical Association, **9**, 209–219 (1905).
- [7] C. W. Gini CW, Variabilità e Mutabilità: Contributo allo Studio delle Distribuzioni e delle Relazioni Statistiche; Cristiano Cuppini: Bologna, Italy (1912).
- [8] J. E. Hirsch, J.E. An index to quantify an individual’s scientific research output, Proc. Natl. Acad. Sci. USA **102**, 16569–16572 (2005).
- [9] A. Ghosh, N. Chattopadhyay and B. K. Chakrabarti, Inequality in societies, academic institutions and science journals: Gini and k-indices, Physica A: Stat. Mech. Appl. **410**, 30–34 (2014).
- [10] A. Ghosh and B. K. Chakrabarti, Limiting value of the Kolkata index for social inequality and a possible social constant. Physica A: Stat.Mech. Appl., **573**, 125944 (2021).
- [11] A. Ghosh and B. K. Chakrabarti, Scaling and kinetic exchange like behavior of Hirsch index and total citation distributions: Scopus-CiteScore data analysis. Physica A: Stat. Mech. Appl. **626**, 129061 (2023).
- [12] S. S. Manna, S. Biswas and B. K. Chakrabarti, Near universal values of social inequality indices in self-organized critical models, Physica A: Stat. Mech. Appl. **2022**, 596, 127121 (2022).
- [13] P. Bak, C. Tang and K. Wiesenfeld, Self-organized criticality: an explanation of $1/f$ noise, Phys. Rev. Lett., **59**, 381 (1987).
- [14] S. S. Manna, Two-state model of self-organized criticality, J. Phys. A: Math. Gen., **24**, L363 (1991).
- [15] A. Ghosh and B. K. Chakrabarti, Do Successful Researchers Reach the Self-Organized Critical Point?, Physics, **6**, 46–59 (2024) (<https://doi.org/10.3390/physics6010004>).
- [16] R. I. M. Dunbar, Neocortex size as a constraint on group size in primates. J. Hum. Evol., **22**, 469–493 (1992).
- [17] Dunbar’s number, Wikipedia (https://en.wikipedia.org/wiki/Dunbar's_number).
- [18] J. Hoshen and R. Kopelman, Percolation and cluster

- distribution. I. Cluster multiple labeling technique and critical concentration algorithm, *Phys. Rev. B* **14**, 3438 (1976).
- [19] J. L. Jacobsen, *J. Phys. A: Math. Theor.*, **48**, 454003 (2015).
- [20] A complete list of percolation thresholds is available in wikipedia (https://en.wikipedia.org/wiki/Percolation_threshold).
- [21] S. S. Manna and R. M. Ziff, Bond percolation between k separated points on a square lattice, *Phys. Rev. E* **101**, 062143 (2020).
- [22] W. Glänzel, On the h-index - A mathematical approach to a new measure of publication activity and citation impact, *Scientometrics*, **67** (2006), pp. 315-321 (2006).
- [23] A. Yong, Critique of Hirsch's Citation Index: A Combinatorial Fermi Problem, *Notices of the American Mathematical Society*, **61**, 1040–1050 (2014). doi: <http://dx.doi.org/10.1090/noti1164>.